

## WAKE FIELDS EFFECTS IN THE SPARC PHOTOINJECTOR

M. Ferrario, V. Fusco<sup>#</sup>, B. Spataro, LNF-INFN, Frascati, Italy  
 M. Migliorati, L. Palumbo, "La Sapienza University", Roma, Italy

### Abstract

When a bunch travels off axis across structures whose shape is not uniform, such as RF cavity or bellows, generates longitudinal and transverse wake fields [1]. In addition transverse time dependent fields (like transverse RF components and wake fields ) may induce correlated slice centroids displacement, so that each slice centroid motion is affected also by a different space charge force generated by the next slices. In this paper the analytical diffraction model for wake fields, developed by Bane and Sands has been implemented in the HOMDYN code taking into account also space charge forces acting on the slice centroids.

As a first application, the preliminary evaluation of the emittance degradation in the SPARC linac when structures are misaligned with respect to the nominal axis is reported.

### WAKE FIELDS DIFFRACTION MODEL

#### Single cavity

When the bunch length  $\sigma$  is much smaller then the beam pipe radius  $a$ ,  $\sigma \ll a$ , methods of diffraction theory [2] are used to calculate the impedance at high frequencies,  $\omega \gg c/a$ , where  $c$  is the velocity of light.

The model suppose each structure as a pill box cavity, whose geometric dimensions are:  $a$  the beam pipe radius,  $b$  the cavity radius and  $g$  its length. When a bunch reaches the edge of the cavity, the electromagnetic field produced is just the one that would occur when a plane wave passes trough a hole; with this hypothesis it is possible to use the classical diffraction theory of optics to calculate the fields.

According to it, the longitudinal and transverse wake fields, in the high energy regime, are respectively [2]

$$W_{||0}(s) = \frac{Z_0 c}{\sqrt{2\pi^2 a}} \sqrt{\frac{g}{s}} \quad (1)$$

$$W_{\perp 0}(s) = \frac{2^{3/2} Z_0 c}{\pi^2 a^3} \sqrt{gs} \quad (2)$$

where  $Z_0$  is the characteristic impedance and  $s$  the longitudinal coordinate inside the bunch, being  $s=0$  the bunch's head.

The above expressions are given for the ultrarelativistic case  $\beta \rightarrow 1$ ; the case of low energy regime was studied in [3-4] where It was shown a dependence of the energy loss and of the wake fields from the relativistic factor  $\gamma$ . However It was shown in [5] that the high energy regime represents an over estimation of the low energy one.

It's worth noting that both the longitudinal and transverse wakes do not depend on the cavity radius  $b$ .

Infact part of the diffracted field, generated when the leading edge of the bunch enters the cavity, will propagate in the cavity; if the bunch's rms length  $\sigma$  is shorter than the cavity radius  $b$ , then the geometrical condition

$$g < \frac{(b-a)^2}{2\sigma}$$

is verified and the scattered field coming from the upper wall of the cavity will never reach the tail of the bunch itself: this is called "cavity regime".

Using Eq. 1 and Eq. 2 as a green function we can calculate the transverse and longitudinal wake field:

$$E_{||}^w(s) = \frac{q}{L} \frac{2}{\sqrt{2\pi^2 a \epsilon_0}} \sqrt{\frac{s}{g}}$$

$$E_{\perp}^w(x, s) = \frac{q}{L} \frac{2^{5/2}}{3\pi^2 a^3 \epsilon_0} \frac{s^{3/2}}{\sqrt{g}} x$$

where  $q$  and  $L$  are the bunch's charge and length respectively.

### BEAM DYNAMICS IN HOMDYN

#### Off-axis beam dynamics

We use the HOMDYN code to study the dynamic of an off axis bunch which travels along structures whose shape is not uniform. The code [6] describes a bunch as a uniformly charged cylinder of charge  $q$  and length  $L$ , divided in cylindrical slices of radius  $R_s$ . The evolution in the time domain of the slice's envelope  $R_s$  is described by its envelope differential equation [6] and the centroid longitudinal position  $z_c$  of each slice is described by

$$\ddot{z}_c = \left\{ \begin{array}{l} \frac{e}{\gamma^3 m} \frac{q}{2\pi \epsilon_0 R_s^2 L \gamma_s} H(\xi_s, R_s, \gamma_s, L) + \\ \frac{e}{\gamma m} E_{||}^w(\xi_s) - \frac{e}{2\gamma m} \left\{ \dot{x}(y B'_z - \sum_i y_{i,off} B'_{z,i}) + \right. \\ \left. - \dot{y}(x B'_z - \sum_i x_{i,off} B'_{z,i}) \right\} \end{array} \right.$$

where  $\xi_s = z_s - z_t$  and  $z_t$  is the bunch's tail.

The first term on the right hand side describes the longitudinal space charge on each slice centroid [5], whilst the wake field is the second term on the right hand side. The remaining terms describe the longitudinal motion in a solenoid field; transverse components of the magnetic fields are approximate with the  $B_z$  derivative.

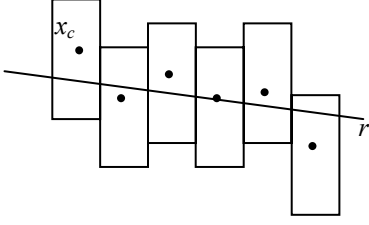


Figure 1: Bunch divided in slices in Homdyn.

In order to describe the displacement of each slice centroid  $x_c$ ,  $y_c$  from the nominal axis of the bunch, it is necessary to include in the code the differential equation describing the centroid motion

$$\ddot{x}_c + \beta\gamma^2 \dot{\beta}\dot{x}_c = \begin{cases} \frac{e}{\gamma^3 m} \frac{q\gamma}{4\pi\epsilon R_s^2 L} d_{xc} G(\xi, R_s, \gamma, L) + \\ + \frac{e}{\gamma m} \left\{ E_{\perp}^w(x_c^1, \xi_s) + \dot{y}B_z + \right. \\ \left. + \frac{1}{2} \dot{z}(yB'_z - \sum_i y_{i,off} B'_{z,i}) \right\} \\ \\ \ddot{y}_c + \beta\gamma^2 \dot{\beta}\dot{y}_c = \begin{cases} \frac{e}{\gamma^3 m} \frac{q\gamma}{4\pi\epsilon R_s^2 L} d_{yc} G(\xi, R_s, \gamma, L) + \\ + \frac{e}{\gamma m} \left\{ E_{\perp}^w(y_c^1, \xi_s) - \dot{x}B_z + \right. \\ \left. - \frac{1}{2} \dot{z}(xB'_z - \sum_i x_{i,off} B'_{z,i}) \right\} \end{cases}$$

Each slice's centroid can be transversally displaced from the nominal axis; in this case it experiences a transverse deflection due to the space charge force produced by the neighbour slices (first term on the right hand side) [6] and the transverse wake force (second term on the right hand side). Finally the last terms describe the beam motion in a solenoid field, including the case of solenoid's coils misalignment  $x_{i,off}$  and  $y_{i,off}$  respect to the nominal axis.

We suppose the transverse wake force on each slice depends on the displacement of the first slice from the axis,  $x_c^1$  or  $y_c^1$  and the space charge on the centroid varies linearly with the distance  $d_{xc}$  or  $d_{yc}$  of the considered slice's centroid from the straight line  $r$  (see Fig. 1). The straight line is obtained interpolating the centroids along the bunch with the least square method.

The space charge on centroids was tested generating a bunch in a case where space charge on centroids is strong; then we compared centroid motion with Parmela results.

### Emittance Computation

The total rms emittance is calculated in the code as follow [6]

$$\mathcal{E}_{not}^2 = (\mathcal{E}_n^{th})^2 + (\mathcal{E}_n^{corr})^2 \quad (3)$$

where  $\mathcal{E}_n^{th}$  is the thermal emittance.

When all the slices lies on the same axis, the correlated emittance is only given by the "envelope" emittance

$$\begin{aligned} (\mathcal{E}_n^e)^2 &= \left\langle \frac{X^2}{4} \right\rangle \left\langle \frac{(\beta\gamma X')^2}{4} \right\rangle - \left\langle \frac{X\beta\gamma X'}{4} \right\rangle^2 = \\ &= \left\langle \frac{a^2}{4} \right\rangle \left\langle \frac{b^2}{4} \right\rangle - \left\langle \frac{ab}{4} \right\rangle^2 \end{aligned}$$

where  $X$  is the slice envelope.

On the contrary if the slices do not lie on the same axis then the correlated emittance is given by the quadratic sum of three terms: the "envelope" emittance mentioned above, the "centroids" and the "cross" emittance, respectively

$$\begin{aligned} (\mathcal{E}_n^c)^2 &= \left\langle (x_c - \langle x_c \rangle)^2 \right\rangle \left\langle (\beta\gamma x_c' - \langle \beta\gamma x_c' \rangle)^2 \right\rangle - \\ &= \left\langle d^2 \right\rangle \left\langle e^2 \right\rangle - \left\langle de \right\rangle^2 \end{aligned}$$

$$(\mathcal{E}_n^{cross})^2 = \left\langle \frac{a^2}{4} \right\rangle \left\langle d^2 \right\rangle + \left\langle \frac{b^2}{4} \right\rangle \left\langle e^2 \right\rangle - 2 \left\langle \frac{ab}{4} \right\rangle \left\langle de \right\rangle$$

where  $\langle \rangle = \frac{1}{S} \sum_1^S$  is performed over the  $S$  slices.

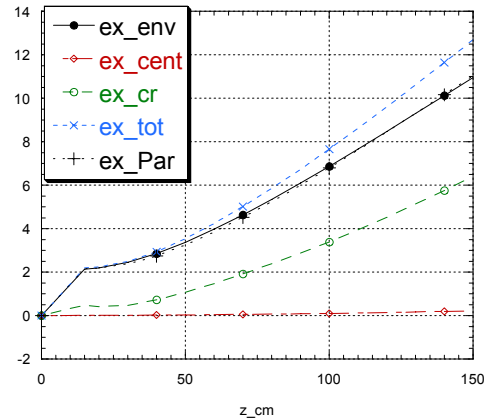


Figure 2: Centroid, cross, envelope and total emittance (light blue line) using Eq. 3, compared with Parmela's emittance results (black crossed line). The bunch is generated with an offset.

The emittance complete expression of an off axis bunch has been inserted in the Homdyn code. Using Parmela's output to obtain slice's envelope and centroid positions, we insert such results in the above equations and calculate analytically the emittance; then we compare the analytical result with the emittance as computed by Parmela. The excellent agreement validates the above computation.

For the Homdyn emittance calculation we assume that the bunch's charge distribution is uniform. The results of

Fig.2 show a good agreement demonstrating the nonlinearities of the space charge force can be neglected.

## EMITTANCE DEGRADATION IN THE SPARC PHOTOINJECTOR

We used the improved version of the Homdyn code described in the previous section to preliminary evaluate the emittance degradation at the end of the travelling wave structures (TW) of the SPARC's project [7].

The bunch is generated on axis whilst the TWs can be transversally displaced with respect to the nominal axis; besides the thirteen coils forming the solenoid of the first TW can be independently displaced as well. We looked for the coils' configuration giving the biggest offset of the bunch's centroid from the nominal axis thus enhancing the wake fields across the bunch. We combined it to a worst configuration for the TWs as specified in Table 1.

Table 1: Solenoid coils and TWs misaligned configuration

Device	$\Delta x$ [mm]	$\Delta y$ [mm]
Solenoid coil 1	0.	+0.1
Solenoid coils 2-3-4-5-6	+0.1	0.
Solenoid coils 7-8-9-10-11-12-13	0.	-0.1
TW1	0.1	0.1
TW2	-0.1	-0.1
TW3	-0.1	-0.1

Finally we corrected the bunch trajectory inserting three steering coils placed at the entrance of each TW structure.

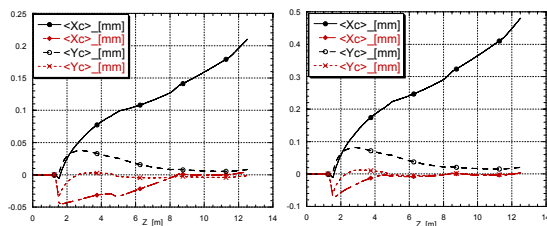


Figure 3: Bunch's centroid position along the structure without (black lines) and with (red lines) steering correction.

Fig.3 shows the bunch centroids positions with and without steerings in the case of the above misaligned configuration for an offset of 0.05mm and 0.1mm. Table2 shows the emittance degradation at the end of the TWs structures whilst Fig.4 shows the emittance behaviour along the structure for the two cases.

It's worth noting the main causes of emittance degradation are the wake fields in the TWs structures. Infact Fig. 5 shows the bunch's emittance when a bunch enters off axis, as an example, in the second TWs structure.

Table 2: Normalized emittance degradation without and with steering correction at the end of the TWs ( $z=12.0m$ ).

Offset	$\epsilon_{nx}$ steer off	$\epsilon_{nx}$ steer on	$\epsilon_{ny}$ steer off	$\epsilon_{ny}$ steer on
0.05mm	1.68 $\mu$ rad	0.84 $\mu$ rad	0.89 $\mu$ rad	0.85 $\mu$ rad
0.1mm	3.47 $\mu$ rad	1.08 $\mu$ rad	1.22 $\mu$ rad	1.06 $\mu$ rad

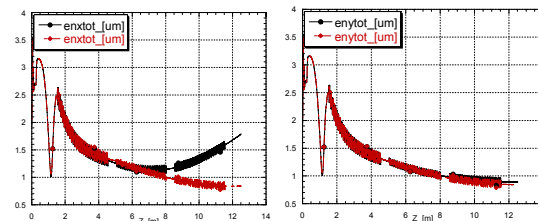


Figure 4: Normalized emittance behaviour along the structure without (black line) and with (red line) steering correction for the case of 0.05mm offset.

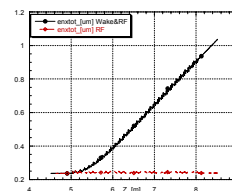


Figure 5: Normalized emittance along the second TW structure for a bunch' offset of 0.1mm when both wake and RF are on (black line) and when only RF is on (red line).

## CONCLUSIONS

The analytical diffraction model for wake fields has been implemented in the Homdyn code; we included space charge force acting on each slice's centroids. As a consequence a new analytical calculation for emittance has been developed and inserted in Homdyn. As a first application, a preliminary evaluation of the emittance degradation and tolerances in the SPARC linac when structures are misaligned respect to the nominal axis, has been studied.

## ACKNOWLEDGEMENT

The authors would like to thank Concetta Ronsivalle for many helpful and interesting discussions.

## REFERENCES

- [1] L. Palumbo et al., "Wake Fields and Impedance", CAS: 5<sup>th</sup> Advanced Accelerator Physics Course.
- [2] K. Bane, M. Sands, SLAC-Pub-4441
- [3] J.D. Lawson, RHEL/M144.
- [4] E. Keil, NIM 100 (1972) 419-427
- [5] H. Henke, CERN-LEP-RF/85-41
- [6] M. Ferrario et al., SLAC-PUB-8400
- [7] D. Alesini et al., "Status of the SPARC Project", this Conference